

Collision-Induced Dissociation Threshold Energies of Protonated Glycine, Glycinamide, and Some Related Small Peptides and Peptide Amino Amides

John S. Klassen and Paul Kebarle*

Contribution from the Department of Chemistry, University of Alberta, Edmonton, Alberta, Canada T6G 2G2

Received August 12, 1996[⊗]

Abstract: The energy thresholds for fragment ions from the collision-induced dissociation of the protonated amino acid glycine (Gly), glycinamides Gly-NH₂ and Gly-NHCH₃, the dipeptides Gly-Gly and Gly-Gly-NH₂, and the peptides Gly-Gly-Gly and Gly-Gly-Gly-Gly were determined with a modified triple quadrupole mass spectrometer. The precursor ions were produced by electrospray. The threshold energies for the formation of the major fragment ions were determined by fitting the experimentally determined threshold curves to theoretical threshold equations following the procedure developed by Armentrout and co-workers. To obtain corrections for the kinetic shifts, several of the transition states were modeled by using *ab initio* or semiempirical calculations. The immonium ion, CH₂NH₂⁺, which is an **a**₁ ion, was observed as a major fragment ion from precursor ions (H₂NCH₂CO-X)H⁺, where X = OH, NH₂, NHCH₃, and NH₂COOH. The activation energies obtained from the thresholds were between 40 and 50 kcal/mol. These energies were in good agreement with theoretically evaluated activation energies for transition states based on a mechanism proposed by Harrison and co-workers. A second pathway leading to XH₂⁺ (**y**₁) ions was observed for X = NHCH₃ and NHCH₂COOH. The threshold based activation energy was somewhat lower than that for the **a**₁ ions. Agreement between the threshold based activation energy and the calculated activation energy for a transition state involving an aziridinone intermediate provides support for the mechanism proposed by Wesdemiotis and co-workers. The lowest energy fragmentation pathway for ions with the general structure ⁺H-(Gly-Gly-X) was found to be the **b**₂ (acylium) ion. In the case where X = NH₂, the activation energy was only 20.4 kcal/mol. This very low energy was found consistent with the **b**₂ ions being cyclic, protonated oxazolones, as proposed by Harrison and co-workers. The thresholds for the fragment ions from larger precursor ions were affected by very large kinetic shifts and suppression by competitive decompositions. Accurate activation energies for these reactions could not be obtained. Nevertheless, the threshold curves provide a view of the evolution into the complex pathways occurring for the higher polypeptides.

I. Introduction

Tandem mass spectrometry (MS/MS) has become an important tool for determining the amino acid sequence of protonated peptides. The technique involves the isolation of the protonated peptide ion in the first stage of mass analysis, excitation of this precursor ion to induce dissociation and mass analysis of the resulting fragment ions. Excitation of the precursor ion is most commonly achieved by energetic collisions with a non-reactive gas, such as argon, and is referred to as collision-induced dissociation (CID). At collision energies readily accessible with triple quadrupole mass spectrometers (<100 eV), protonated peptides dissociate primarily along the backbone at the amide bonds producing **b** ions which contain the N-terminus and are formally acylium ions, H(-HNCHRCO-)_n⁺, and **y** ions which contain the C-terminus and correspond to protonated peptides or amino acids.¹ Theoretical results² suggest that these reactions are charge directed, involving protonation of the amide nitrogen at the site of cleavage. In a typical CID experiment the average internal energy deposited in the precursor ion is chosen to be much larger than the activation energies required for a single dissociation and, as a result, the primary fragment ions themselves undergo fragmentation, producing smaller **a**, **b**, and **y** ions. Decomposition of the **b** ions results in the formation

of smaller **b** ions as well as immonium ions (**a** ions) which are also commonly observed in the low-energy CID spectra of peptides.^{3,4} Sequence information is obtained from the mass difference of successive fragment ions of the same type (e.g. **b**_n-**b**_{n-1}), which corresponds to the mass of the residue by which they differ. The amount of sequence information available from an MS/MS experiment, therefore, depends on the type of fragment ions that are generated and the range of the residues that they include.

Despite the importance and widespread use of CID-MS to sequence peptides, the mechanistic details of the dissociation processes are poorly understood. A better understanding of major dissociation pathways and the effects of primary and higher order structure on these reactions is of interest not only from a fundamental point of view but also for practical reasons, such as for future refinements of CID-MS as a sequencing technique. This lack of mechanistic information is due in large part to the scarcity of experimentally determined dissociation energetics, a deficiency that is currently being addressed by a few research groups. Meot-Ner and co-workers have recently determined the activation energy for the dissociation of protonated leucine enkephalin by measuring the temperature dependence for the decomposition of the protonated peptide ion in a heated capillary flow reactor interfaced with a mass spectrom-

[⊗] Abstract published in *Advance ACS Abstracts*, July 1, 1997.

(1) Hunt, D. F.; Yates, J. R., III; Shabanowitz, J.; Winston, S.; Hauer, C. R. *Proc. Natl. Acad. Sci. U.S.A.* **1986**, *83*, 6233.

(2) Somogyi, A.; Wysocki, V. H.; Mayer, I. *J. Am. Soc. Mass Spectrom.* **1994**, *5*, 704.

(3) Poppe-Schriemer, N.; Ens, W.; O'Neil, J. D.; Spicer, V.; Standing, K. G.; Westmore, J. B.; Yee, A. A. *Int. J. Mass Spectrom. Ion Processes.*

(4) Yalcin, T.; Khow, C.; Csizmadia, I. G.; Peterson, M. R.; Harrison, A. G. *J. Am. Soc. Mass Spectrom.* **1995**, *6*, 1164.

eter.⁵ The flow reactor was operated at a pressure close to 1 atm, which allowed for the activation energy to be measured in the high-pressure limit. Williams and co-workers are presently investigating a promising new technique for studying the temperature dependence of the dissociation kinetics of large biomolecules in which the precursor ions are heated via blackbody infrared radiation inside an ICR cell.⁶

An on-going area of research in our laboratory involves the application of energy-resolved CID-MS,^{7,8} developed by Armentrout and co-workers, to measure the dissociation threshold energies of ions generated by electrospray (ES). Our original interest in this technique was as an alternative to the ion-equilibrium method⁹ for measuring ion–ligand binding energies for complexes generated by ES.¹⁰ Using the CID threshold method, we have recently measured the sodium and potassium ion affinities of several amides as well as glycine and glycyglycine.¹¹ In the present work, we apply this technique to determine the appearance curves of the dominant, low-energy CID fragment ions of several protonated peptides and their amino amides. The resulting appearance curves not only provide qualitative insight into the dissociation process but also can lead to determinations of the activation energies, *i.e.* the energy differences between the precursor ion and the transition state involved in the formation of a given fragment ion. The activation energies are assumed equal to the threshold energies, E_0 , which are obtained from the appearance curves by curve-fitting procedures (*vide infra*). The E_0 values can then be compared with activation energies obtained from quantum mechanical calculations, where the transition state modeled is a transition state corresponding to a given proposed mechanism for the dissociation reaction. Agreement between the two values will then represent strong support for the validity of the proposed mechanism. Evidently, the success of this approach will depend on the accuracy of the experimental and theoretical determinations. Theoretical computation with large basis sets becomes very costly for large molecules, and therefore the present approach can be realistically applied only to amino acids and di- and tripeptides. As will be seen, the evaluation of the activation energies E_0 from the threshold curves becomes more difficult as the size of the peptide increases so that a limitation to small peptides is imposed also to the determinations based on the threshold curves. The theoretical calculations performed in the present work employed only low-level basis sets or semiempirical methods. These results fall short of the accuracy required to establish the reaction mechanism. Nevertheless, the results are interesting and we hope that the availability of the data obtained will stimulate theoretical work by researchers specialized in that area.

II. Experimental and Data Treatment

a. Apparatus and Conditions for Ion Thermalization. The present measurements were performed with a modified SCIEX Trace

(5) Meot-Ner, M.; Dongre, A. R.; Somogyi, A.; Wysocki, V. H. *Rapid Commun. Mass Spectrom.* **1995**, *9*, 829.

(6) Price, W. D.; Schnier, P. D.; Williams, E. R. *Anal. Chem.* **1996**, *68*, 859.

(7) Armentrout, P. B. Thermochemical Measurements by Guided Ion Beam Mass Spectrometry. In *Advances in Gas Phase Ion Chemistry*; Adams, N., Babcock, L. M., Eds.; JAI Press Inc., Greenwich, CT, 1992; Vol. 1, p 83.

(8) (a) Sunderlin, L. S.; Wang, D.; Squires, R. R. *J. Am. Chem. Soc.* **1993**, *115*, 12060. (b) Mazinelli, P. J.; Paulino, J. A.; Sunderlin, L. S.; Wenthold, P. G.; Poutsma, J. C.; Squires, R. R. *Int. J. Mass Spectrom. Ion Processes* **1994**, *130*, 89. (c) Magnera, T. F.; David, D. E.; Stulik, D.; Orth, R. G.; Jonkman, H. T.; Michl, J. *J. Am. Chem. Soc.* **1989**, *111*, 5036.

(9) Kebarle, P. *Annu. Rev. Phys. Chem.* **1977**, *28*, 445.

(10) (a) Klassen, J. S.; Blades, A. T.; Kebarle, P. *Phys. Chem.* **1995**, *99*, 15509. (b) Blades, A. T.; Klassen, J. S.; Kebarle, P. *J. Am. Chem. Soc.* **1995**, *117*, 10563.

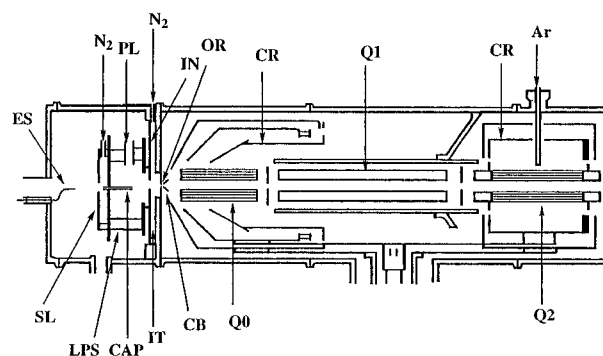


Figure 1. Front end of apparatus. Electrospray generator, ES, consisting of electrospray capillary with stainless steel tip at high electric potential. ES generates charged droplets and ultimately gas-phase ions. ES is partially surrounded by a glass tube providing a flow of dry air. The capillary, CAP, transfers gas and ions from 1 atm to a low pressure ion source, LPS, maintained at 10 Torr. Ions can be partially declustered by applying a high drift field between the CAP and the interface plate, IN. Ions are allowed to rethermalize in a low drift field ion thermalization chamber, IT. The orifice, OR, leads to a vacuum. The first electrode/skimmer, CB; RF only ion guide quadrupole, Q0; first quadrupole, Q1. Cryosurfaces, CR, for cryopumping.

Atmospheric Gas Analyzer (6000E) triple quadrupole mass spectrometer that has been described previously¹¹ and only a brief description is given here. The modified front end of the mass spectrometer is shown in Figure 1.

The gas-phase ions were generated by electrospraying methanol solutions containing 10^{-3} – 10^{-4} M peptides and 10^{-4} M HCl. The ions are transferred from atmospheric pressure into the low-pressure source (LPS) via a stainless steel capillary (CAP, 3.5 cm long, 0.33 mm i.d.). The pressure in the LPS is maintained at 10 Torr by means of a pump. Protonated peptides (MH^+) generated by ES are often clustered with water or solvent molecules ($MH^+(H_2O)_n(MeOH)_m$). Some initial declustering of the ions is obtained by reducing the partial pressure of H_2O and $MeOH$ in the LPS. This is achieved at the atmospheric side of CAP by flowing dry N_2 (~ 1 L/min) around the CAP, where the N_2 flow is countercurrent to the ES plume. Additional declustering is obtained by applying a high ion drift field between the tip of the CAP (200–400 V) and the bottom plate, IN (110 V). A weak drift field ($E/P < 2$ V cm^{-1} Torr $^{-1}$) between IN and the orifice, OR (100 V), *i.e.* in the ion thermalization chamber which contains N_2 gas at 10 Torr, ensures that the ions reach OR with thermal energies. In order to avoid collisional heating during sampling into the mass spectrometer, OR, CB, and Q0 were set at equal potentials (100 V). Precursor ions are mass selected with the first quadrupole (Q1) and accelerated to a known kinetic energy by selecting a suitable offset potential for the radio frequency only quadrupole (Q2), which serves as the collision cell. Argon was used as the collision gas. The fragment ions produced in Q2 are mass analyzed by the third quadrupole (Q3) and detected with an ion counting system.

Tests were performed to establish that the threshold value E_0 for a given product ion, see section b, is independent of the declustering drift field applied between CAP and IN. Changes of the CAP to IN potential from 260 V to 190 V led to changes of E_0 for the immonium ion from protonated glycine (Table 1) of only ~ 0.04 eV. These changes were within the reproducibility range of E_0 determinations obtained with constant voltage parameters. For another similar test, see previous work.^{11b}

The drift field in the thermalization chamber between IN and OR is very weak, $E/P \leq 2$ V cm^{-1} Torr $^{-1}$. According to experiments by Castleman *et al.*,¹² drift fields where $E/P < 15$ V cm^{-1} Torr lead to ions with near thermal energies. The residence time of the ions in the weak drift region which is 5 mm long is difficult to estimate because the ions not only drift but are also carried by the plume of the gas

(11) (a) Klassen, J. S.; Anderson, S. G.; Blades, A. T.; Kebarle, P. *J. Phys. Chem.* **1996**, *100*, 14218. (b) Anderson, S. G.; Blades, A. T.; Klassen, J. S.; Kebarle, P. *Int. J. Mass Spectrom. Ion Processes* **1995**, *141*, 217.

(12) Keesee, R. G.; Lee, N.; Castleman, A. W., Jr. *J. Am. Chem. Soc.* **1979**, *101*, 2599.

Table 1. CID Threshold Energies (E_0)^a

precursor ion (MH ⁺)	fragment ion	E_0^b		E_0^c		ΔS^\ddagger ^d
		eV	(kcal/mol)	eV	(kcal/mol)	
⁺ H ₃ NCH ₂ COOH	⁺ H ₂ N=CH ₂ (a1)	1.90 ± 0.07	(43.9)	1.93	(44.4)	10.4
⁺ H ₃ NCH ₂ CONH ₂	⁺ H ₂ N=CH ₂ (a1)	1.92 ± 0.11	(44.2)	1.95	(44.9)	12.8
⁺ H ₃ NCH ₂ CONHCH ₃	⁺ H ₂ N=CH ₂ (a1)	2.16 ± 0.19	(49.9) ^e	2.61	(60.0)	5.8
⁺ H ₃ NCH ₂ CONHCH ₃	⁺ H ₃ NCH ₃ (y1)	2.10 ± 0.23	(48.5)	2.60	(59.8)	4.6
		(2.16) ^e	(49.9) ^e			(5.8) ^e
(Gly-Gly)H ⁺	⁺ H ₂ N-CH ₂ (a1)	1.89 ± 0.26	(43.7)	2.81	(64.9)	-3.2
(Gly-Gly)H ⁺	⁺ H ₃ NCH ₂ COOH (y1)			2.35	(54.1)	
(Gly-Gly-NH ₂)H ⁺	MH ⁺ -NH ₃ (b2)	0.88 ± 0.21	(20.4)	0.93	(21.4)	3.8
(Gly-Gly-NH ₂)H ⁺	MH ⁺ -(CO+NH ₃) (a2)			2.99	(69.0)	
(Gly-Gly-NH ₂)H ⁺	MH ⁺ -GlyNH ₂ (y1)			2.99	(69.0)	
(Gly-Gly-NH ₂)H ⁺	⁺ H ₂ N-CH ₂ (a1)			3.57	(82.3)	
(Gly-Gly-Gly)H ⁺	MH ⁺ -Gly (b2)			2.36	(54.5)	
(Gly-Gly-Gly)H ⁺	(Gly-Gly)H ⁺ (y2)			3.17	(73.1)	
(Gly-Gly-Gly-Gly)H ⁺	MH ⁺ -Gly ₂ (b2)			3.43	(79) ^f	
(Gly-Gly-Gly-Gly)H ⁺	(Gly-Gly)H ⁺ (y2)			2.73	(63) ^f	

^a Threshold energies (E_0) in eV and (kcal/mol). Error limits are given only for values quoted in eV. Only values for which error limits are given have thermochemical significance. For evaluation of error limits see section d, Experimental and Data Treatment. ^b Threshold energies, obtained with eq 2, include correction for kinetic shift. ^c Threshold energies obtained with eq 1, with no correction for kinetic shift. ^d ΔS^\ddagger values are calculated at 1000 K, in units of cal/(mol K). ^e Upper limit for threshold energy obtained by using vibrational frequencies of the transition state of the complementary **a1** ion. ^f Average internal energy of precursor estimated to be 10.0 kcal/mol.²⁶

which exits the capillary CAP. Threshold energy, E_0 , determinations for the immonium ion from protonated glycine were also performed with a different source normally used for ion-equilibria determinations.^{10a} In this "side-on" source, the gas plume and ions from CAP enter slightly above and parallel to the IN plate. Otherwise, the source is identical with the present one. The ions are deflected by a weak field such that some of them enter the ion thermalization chamber IT. For the same drift field, 2 V cm⁻¹ Torr⁻¹, the residence time in IT has been estimated as ~100 μ s.^{10a} Some 10⁵ collisions with the 10 Torr pressure buffer gas N₂ can be expected to occur in IN-OR. Therefore, these ions are certainly thermalized. Threshold curves can be measured with that source even though the precursor ion intensities are lower by a factor of ~10. The threshold for the **a1** ion from protonated glycine was only 0.05 eV lower than the value obtained with the "straight-on" source of the present work.

b. Determination of Threshold Energies, E_0 , and Kinetic Shifts. The threshold energies, E_0 , were obtained by fitting the fragment ion appearance curves with eq 1, using the CRUNCH program developed by Armentrout and co-workers,^{13a}

$$\sigma = \sigma_0 \sum_i g_i (E + E_i - E_0)^n / E \quad (1)$$

where E is the collision energy (in the center of the mass frame, CM), E_0 is the threshold energy, and E_i is the vibrational energy of a given vibrational state with a relative population given by g_i . The temperature of the precursor ions was assumed to be 298 K. σ_0 is a scaling factor and n is a variable parameter; both are optimized during the fitting procedure, along with E_0 .

An underlying assumption in eq 1 is that any precursor ion with an internal energy greater than E_0 will decompose inside the collision cell (Q2) prior to reaching the mass analyzer (Q3). The residence time (t) in Q2 can be estimated and is between 20 and 40 μ s for the present ions. For precursor ions with many degrees of freedom, additional internal energy is required to achieve a dissociation rate constant large enough to ensure that fragmentation occurs within the residence time (t) prior to the ions entering Q3. This additional energy is referred to as a kinetic shift, and if not taken into account, it will lead to E_0 values that are too high. A modified version of eq 1 available in the CRUNCH program^{13b} allows for lifetime effects to be considered explicitly. This is done by calculating the unimolecular rate constants for a given dissociation process as a function of internal energy of the precursor ion, according to the RRKM formalism. On the basis of these rate constants, the probability (P) that a precursor ion with an initial translational energy (E) and internal energy (E_i) will decompose within

the given experimental window (t) can be evaluated and eq 1 is scaled accordingly (see eq 2).

$$\sigma = \sigma_0 \sum_i [g_i P(E, E_i, t) (E + E_i - E_0)^n / E] \quad (2)$$

c. Theoretical Calculations: Precursor Ion and Transition State.

The vibrational energy distribution of the precursor ions, required for eqs 1 and 2, was obtained from calculated normal vibrational modes. Geometry optimization and hessian analysis was carried out with low-level *ab initio* or semiempirical methods available in the GAMESS program.¹⁴ Evaluation of the unimolecular dissociation rate constants (RRKM), used in eq 2 to account for lifetime effects, requires also the vibrational frequencies of the transition state. Where possible the transition states were modeled theoretically. Details of the methods used to locate the transition states are given in the Results and Discussion section.

d. Data Analysis, Threshold Curve Fitting, and Instrumental Limitations Responsible for Errors in Threshold Energy, E_0 , Determinations. The threshold curves for the product ions were determined at Ar collision gas pressures of ≤ 0.05 mTorr (collision cell length 15 cm). At the selected pressure, the intensity of the fragment ion, when at its maximum, was less than 3% and generally close to 1% of the intensity of the precursor ion. Generally 100 to 200 scans over the threshold curve energy range for a given product ion were collected and then averaged to obtain the experimental points shown in the threshold curves, Figures 2, 4, and 6–10.

The product ion intensities leading to the threshold curves were not expressed as cross sections and in particular were not divided by the precursor ion intensity. The precursor ion intensity observed with triple quadrupole instruments exhibits a fluctuation of intensity with ion velocity due to quadrupole focussing effects, see Figure 2 in Magnera,^{8d} and this makes the normalization to the precursor ion intensity not desirable.^{8d}

Threshold values obtained from repeated experimental determinations of a threshold curve showed a reproducibility within ± 0.05 eV, even when repeat experiments separated by a month were performed.

The zero of the energy scale was obtained by fitting a Gaussian function to the derivative of the precursor ion retarding curve. The zero point was taken at the maximum of the Gaussian function. This zero value was generally within a few tenths of an eV (lab) of the nominal zero energy, *i.e.* $V(\text{OR}) - V(\text{Q2}) = 0$. The width of the Gaussian curve (fwhm) was generally 1.5 eV (lab) or less, see also previous work.^{11b}

(13) (a) Dalleska, N. F.; Honma, K.; Armentrout, P. B. *J. Am. Chem. Soc.* **1993**, *115*, 12125. (b) Loh, S. K.; Hales, D. A.; Lian, L.; Armentrout, P. B. *J. Phys. Chem.* **1989**, *90*, 5466.

(14) Schmidt, M. W.; Baldrige, K. K.; Boatz, J. A.; Elbert, S. T.; Gordon, M. S.; Jensen, J. H.; Koseki, S.; Matsunaga, N.; Nguyen, K. A.; Su, S. J.; Windus, T. L.; Dupuis, M.; Montgomery, J. A. *J. Comput. Chem.* **1993**, *14*, 1347.

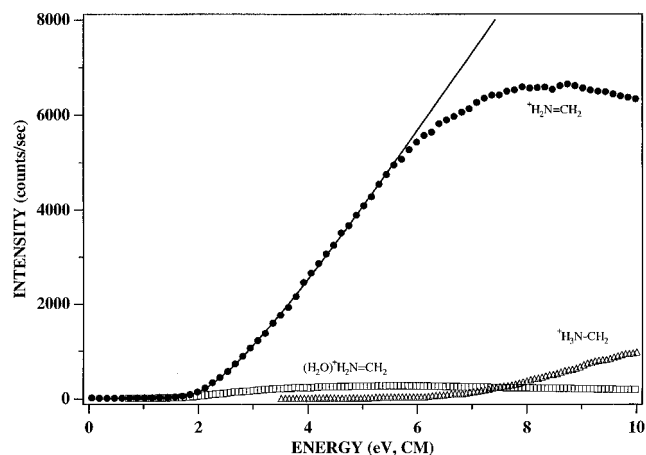


Figure 2. Appearance curves of $^+\text{H}_2\text{N}=\text{CH}_2$ (●), $(\text{H}_2\text{O})^+\text{H}_2\text{N}-\text{CH}_2$ (□), and $^+\text{H}_3\text{N}-\text{CH}_2$ (Δ) from CID of $(\text{Gly})\text{H}^+$. The calculated curve (solid line), fitted from 2.5 to 6.0 eV, corresponds to $n = 1.82$ and $E_0 = 1.93$ eV (44.4 kcal/mol) (eq 1).

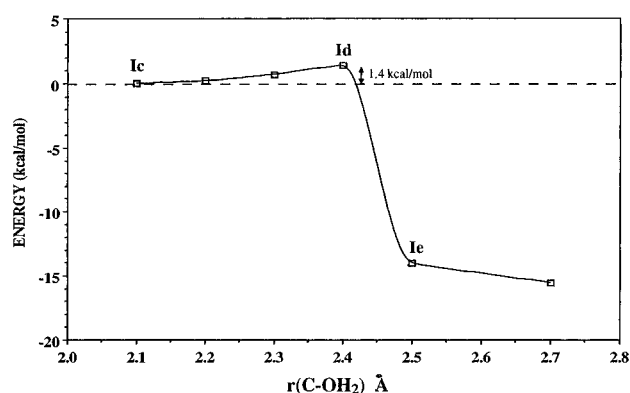


Figure 3. Calculated HF energy (3-21G basis set) of $(\text{Gly})\text{H}^+$, with the proton located on the hydroxyl group, as a function of the C–OH₂ bond length. The energies are scaled relative to the calculated energy of **Ic**, which is taken as 0 kcal/mol. The maximum energy (1.4 kcal/mol) occurs at a bond length of 2.4 Å (**Id**).

In the previous CID threshold work¹¹ with the present apparatus, it was observed that the kinetic energy profile of the precursor ion had a tail toward higher kinetic energies. This broadening was found to increase as the radial DC field in the first quadrupole Q1 was increased. Collisions of the precursor ions with neutral gas molecules of the gas jet originating at OR and extending into Q1 were assumed to be responsible for the broadening.^{11b} The broadening was reduced by working at low radial DC fields in Q1, *i.e.* at low mass resolution in Q1. It was also found^{11a} that the broadening could be further reduced by selecting a specific offset potential for Q1, *i.e.* by controlling the axial kinetic energy of the precursor ions in Q1. Both of these two measures were applied in the present work to reduce the kinetic energy broadening. However, the higher radial DC values required for higher mass precursor ions were still found to lead to increasing broadening with precursor ion mass. Therefore, the threshold curves for the product ions from the higher mass precursor ions could not be fitted with eqs 1 and 2 right down to the onset, *i.e.* a range of points had to be omitted; compare the fit of the product ion CH_2NH_2^+ from low mass precursor ion $(\text{Gly})\text{H}^+$ where the complete threshold could be fitted, Figure 2, with the fit for the same product ion from $(\text{Gly}-\text{Gly})\text{H}^+$ where the tail of the onset was not fitted, Figure 7.

For the **a**₁ ion from $(\text{Gly})\text{H}^+$, Figure 2, essentially identical E_0 values were obtained from fits including points from 1.5–6 eV and 2.5–6 eV, but fits from the same lower limit extending only to 5 eV gave an E_0 lower by 0.04 eV. For this ion we assign 0.05 eV as the curve fitting error. For a summary of assigned errors to a given threshold determination see the end paragraph of this section.

The product ion curves fitted for the $(\text{GlyNH}_2)\text{H}^+$ and $(\text{GlyNHCH}_3)\text{H}^+$ precursor ions, Figures 4 and 6, do not provide a good fit for the

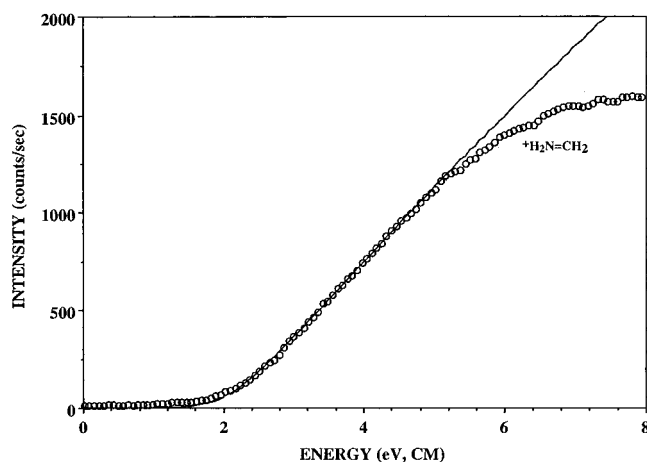


Figure 4. Appearance curves of $^+\text{H}_2\text{N}=\text{CH}_2$ from CID of $(\text{GlyNH}_2)\text{H}^+$. The calculated curve (solid line), fitted from 2.5 to 6.0 eV, corresponds to $n = 1.65$ and $E_0 = 1.95$ eV (44.9 kcal/mol) (eq 1).

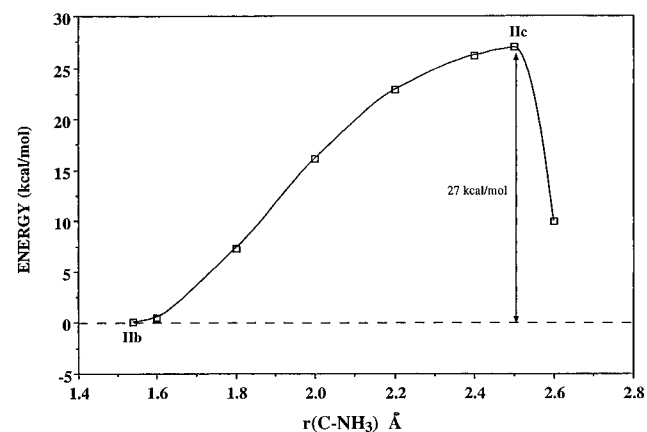


Figure 5. Calculated HF energy (3-21G basis set) of $(\text{GlyNH}_2)\text{H}^+$, with the proton located on the amide nitrogen, as a function of the OC–NH₃ bond length. The energies are scaled relative to the calculated energy of **Iib**, which is taken as 0 kcal/mol. The maximum energy (27.0 kcal/mol) occurs at a bond length of 2.5 Å (**Iic**).

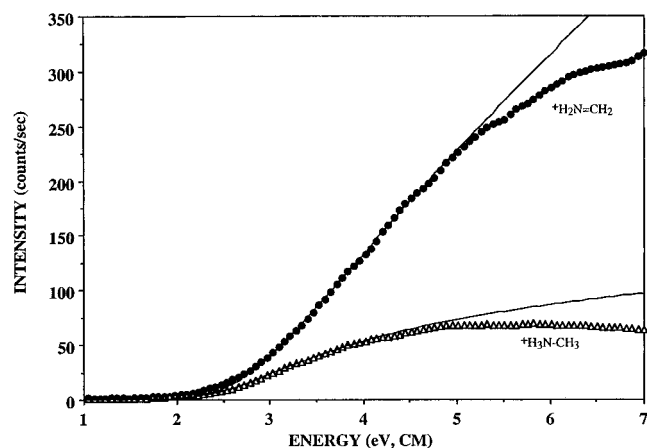


Figure 6. Appearance curves of $^+\text{H}_2\text{N}=\text{CH}_2$ (●) and $^+\text{H}_3\text{NCH}_3$ (Δ) from CID of $(\text{GlyNHCH}_3)\text{H}^+$. The calculated curves (solid lines), fitted from 3.0 to 5.0 eV for $^+\text{H}_2\text{N}=\text{CH}_2$ and 2.5 to 3.5 eV for $^+\text{H}_3\text{NCH}_3$, correspond to $n = 1.54$ and $E_0 = 2.61$ eV (60.0 kcal/mol) and $n = 1.07$ and $E_0 = 2.60$ (59.8 kcal/mol), respectively (eq 1).

experimental points at lowest energies. When these points were included, the E_0 values obtained were lower by ~0.1 eV. Therefore, for these ions we assign 0.1 eV as the curve fitting error.

The product ions from the higher mass $\text{Gly}-\text{Gly}$, Figure 7, and $\text{Gly}-\text{GlyNH}_2$, Figure 8, were fitted only above the low-energy tail, *i.e.* starting with the steeply rising portion. The error introduced by this

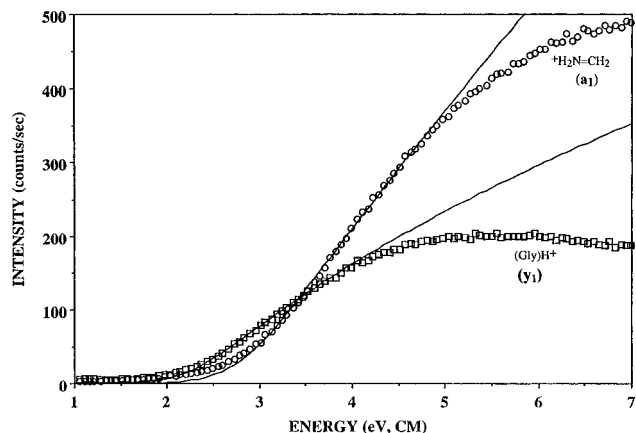


Figure 7. Appearance curves of $^+\text{H}_2\text{N}=\text{CH}_2$ (O) and $(\text{Gly})\text{H}^+$ from CID of $(\text{Gly-Gly})\text{H}^+$. The calculated curves (solid lines), fitted from 3.0 to 5.0 eV for $^+\text{H}_2\text{N}=\text{CH}_2$ and 2.5 to (eq 2) for $(\text{Gly})\text{H}^+$, correspond to $n = 1.78$ and $E_0 = 1.87$ eV (43.0 kcal/mol) and $n = 1.34$ and $E_0 = 2.35$ eV (54.1 kcal/mol), respectively (eq 1).

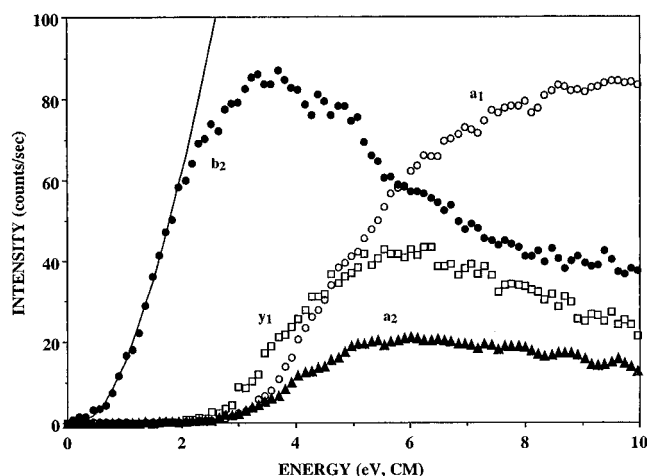


Figure 8. Appearance curves of the b_2 (●), a_2 (▲), y_1 (□), and a_1 (○) fragment ions from CID of $(\text{Gly-GlyNH})\text{H}^+$. The calculated curve (solid line) for the b_2 ion, fitted from 1.0 to 2.5 eV, corresponds to $n = 1.52$ and $E_0 = 0.93$ eV (21.4 kcal/mol) (eq 1).

procedure was estimated by making a comparison with threshold curves where a complete fit could be obtained, e.g. Figure 2. For the Figure 2 data when one started at the steeply rising portion by fitting the range 3.0–6 eV, a higher threshold ($E_0 = 2.11$ eV, $n = 1.68$) was obtained. The difference between the two results, 0.2 eV, was taken as the uncertainty introduced by the omission of the low-energy tails in the thresholds, Figures 7 and 8.

The curve-fitting error for product ions from the higher mass precursor ions Gly-Gly-GlyH^+ and $\text{Gly-Gly-Gly-GlyH}^+$, Figures 9 and 10, is probably higher than ± 0.2 eV. No quantitative thresholds (eq 2) have been quoted for these ions.

The calculated vibrational frequencies for the precursor ion and the transition state can be in error. Each set of vibrational frequencies were multiplied by factors of 0.75 and 1.25, and the spread of E_0 values obtained with eq 1 was taken as the uncertainty due to the precursor ion frequencies, while that for eq 2 was taken as the error due to the transition state frequencies.

The time t available for the decomposition of the energized precursor ions before mass analysis in Q3 was estimated on the basis of the equation: $E_{\text{trans}} = E_0(M_{\text{ion}}/M_{\text{Ar}})$, where E_{trans} is the kinetic energy in the axial direction of the collision pair, ion + Ar, which are assumed to travel with the same speed. This condition holds for collisions at the threshold, where the conversion of kinetic to internal energy is maximum. E_0 is the threshold energy determined with eq 1. The time t equals d/v , where d is the average distance for the flight and v is the velocity of the ion–argon collision pair evaluated with E_{trans} . Taking $d = 7.5$ cm (half the Q2 length), t values were obtained for all product

ions whose E_0 , eq 2, was to be evaluated. The times obtained varied from 23 μs for a_1 from Gly-GlyH^+ to 39 μs for b_2 from Gly-Gly-NH_3^+ . The error due to uncertainty in t was estimated by doing threshold fits with eq 2 and changing t by $\pm 25\%$. The errors were very small, ± 0.02 eV for the case with the largest kinetic shift, a_1 from Gly-GlyH^+ .

The evaluated uncertainties in electronvolts (for curve fitting error; vibrational frequencies; time; and reproducibility) are listed below for each product ion: a_1 from GlyH^+ (0.05; ~ 0.01 ; ~ 0.01 ; 0.05); a_1 from GlyNH_2H^+ (0.17; ~ 0.01 ; ~ 0.01 ; 0.05); a_1 from $\text{Gly-NHCH}_3\text{H}^+$ (0.15; 0.1; 0.03; 0.05); y_1 from $\text{GlyNH}_2\text{CH}_3\text{H}^+$ (0.2; 0.1; 0.03; 0.05); a_1 from Gly-GlyH^+ (0.2; 0.15; 0.04; 0.05); and b_2 from $\text{Gly-GlyNH}_2\text{H}^+$ (0.2; 0.01; 0.01; 0.05). The total error estimate obtained with the chain rule is given in Table 1 for each of the above ions. For example, the uncertainty for the a_1 ion from Gly-GlyH^+ is obtained from $(0.2^2 + 0.15^2 + 0.04^2 + 0.05^2)^{1/2} = \pm 0.26$.

The largest error is due to the threshold tailing, and this error increases as the mass of the precursor ion increases. The effect with increasing mass is probably due to two contributing factors: (a) the increasing radial DC field in Q1, see previous work;^{11b} and (b) the increasing cross section for vibrational excitation of the peptide precursor ions. Due to the tailing problem, the quality of the threshold curves and E_0 values obtained is lower than that obtained with the Guided Ion Beam apparatus used by Armentrout and co-workers.⁷

III. Results and Discussion

a. CID of $^+\text{H}(\text{H}_2\text{NCH}_2\text{COX})$, where X = OH, NH₂, NHCH₃. Mechanism and Energy Changes of Processes Leading to the Immonium Ion, $\text{H}_2\text{N}=\text{CH}_2^+$. Protonated glycine was chosen as the starting point of the present study because this compound is the simplest constituent of peptides. Glycinamide (X = NH₂) and particularly glycine methylamide (X = NHCH₃) are compounds which may be used as the simplest models of peptides. Furthermore, a wealth of experimental^{15,16} and theoretical¹⁷ information is available in the literature on the gas-phase chemistry of protonated amino acids and protonated glycine. It was felt that combining the information gained from the present threshold studies with the insights provided from the literature^{15–17} for glycine, glycinamide, and glycine methylamide may lead to an essential understanding of the basic fragmentation mechanisms and energetics and provide the key to the backbone fragmentation mechanisms of oligopeptides.

The appearance curves from CID of protonated glycine show at a collision energy of 10 eV lab (3.4 eV (CM)) the immonium ion $^+\text{H}_2\text{N}=\text{CH}_2$ (m/z 30) as the major product with a small amount of the immonium ion–water complex (m/z 48) (Figure 2). These fragment ions have been previously observed in the metastable ion spectrum of FAB-generated protonated glycine,^{16b} wherein the hydrate was observed as the dominant fragment ion. At higher collision energies (> 6 eV (CM)), a new minor reaction pathway is observed, leading to the formation of a fragment ion at m/z 31 (CH_5N^+). This ion has been observed in high-energy CID experiments and has been identified on the basis of MS/MS as the distonic ylide ion ($^+\text{H}_3\text{N}-\text{CH}_2^*$).^{16b}

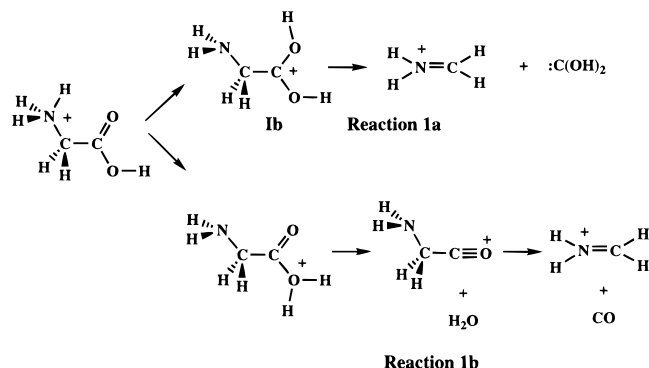
The threshold obtained for the immonium ion is given in Table 1. The thresholds for the other two ions could not be

(15) (a) Meot-Ner, M.; Field, F. H. *J. Am. Chem. Soc.* **1973**, *95*, 7207. (b) Tsang, C. W.; Harrison, A. G. *J. Am. Chem. Soc.* **1976**, *98*, 1301. (c) Doorkeran, N. N.; Yalcin, T.; Harrison, A. G. *J. Mass Spectrom.* **1996**, *31*, 500.

(16) (a) Cordero, M. M.; Houser, J. J.; Wesdemiotis, C. *Anal. Chem.* **1993**, *65*, 1594. (b) Beranova, S.; Cai, J.; Wesdemiotis, C. *J. Am. Chem. Soc.* **1995**, *117*, 9492.

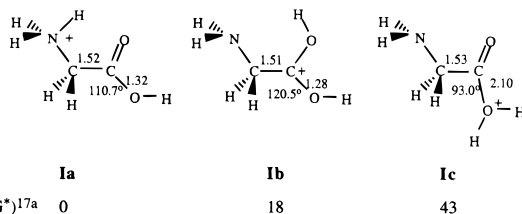
(17) (a) Bouchonnet, S.; Hoppilliard, Y. *Org. Mass Spectrom.* **1992**, *27*, 71. (b) Jensen, F. *J. Am. Chem. Soc.* **1992**, *114*, 9533. (c) Bouchoux, G.; Bourcuis, S.; Hoppilliard, Y.; Mauriac, C. *Org. Mass Spectrom.* **1993**, *28*, 1064.

Scheme 1



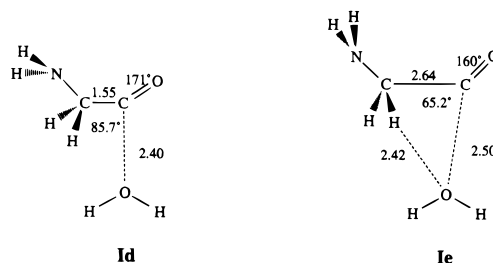
determined accurately; however, the onset regions observed provide useful qualitative information as will be shown below.

Formation of the immonium ion, the dominant fragment ion over the energy range studied, formally involves the loss of CO_2H_2 . The most direct route leading to the immonium ion would involve proton transfer from the amino group to the carbonyl oxygen, followed by heterolytic bond cleavage and loss of the dihydroxycarbene neutral (Scheme 1, reaction 1a). An alternative mechanism, proposed by Tang and Harrison,^{15b} proceeds by protonation of the hydroxyl group followed by the loss of H_2O and CO (reaction 1b). The acylium ion ($\text{H}_2\text{N}-\text{CH}_2-\text{CO}^+$) intermediate has not been detected mass spectrometrically, and evidence was presented that it is unstable with respect to the loss of CO .^{15b} Using heats of formation of the precursor ion and the final products taken from the literature, Beranova *et al.*^{16b} have recently evaluated the overall reaction endothermicities for the two reaction pathways. Reaction 1a, leading to the dihydroxycarbene, is found to be 64 kcal/mol endothermic, while reaction 1b is predicted to be 33 kcal/mol endothermic. Although no heats of formation are available for the transition states for the reactions shown in Scheme 1, useful related estimates are provided by Hoppilliard and co-workers,^{17a} who have calculated the relative energies (MP2/6-31G**//3-21G) (not including zero point energy corrections) of the isomeric forms of protonated glycine (**Ia**, **b**, and **c**). Protonation of the amino group (**Ia**) is calculated to be 18 kcal/mol more stable than protonation of the carbonyl oxygen (**Ib**) and 43 kcal/mol more stable than protonation of the hydroxyl group (**Ic**). The calculations also reveal that protonation of the hydroxyl group results in an unusually long C—OH₂ bond (2.1 Å) such that **Ic** resembles an acylium ion—water complex. On the basis of these values,^{17a} a lower limit of 43 kcal/mol, corresponding to the proton transfer from the amino to the hydroxyl group, can be assigned to the energy barrier for the formation of the transition state of reaction 1b. The final products from this reaction are predicted^{16b} to lie 35 kcal/mol below the energy of **Ic**.



Fitting the immonium ion appearance curve, Figure 2, with eq 1 gives a threshold energy of 44.4 kcal/mol (see Table 1). As discussed in the Experimental Section, the threshold energy obtained with eq 1 assumes that there is no kinetic shift present and therefore can be viewed as an upper limit of the true

threshold energy. A more reliable value is obtained when lifetime effects are explicitly considered. In order to evaluate the RRKM rate constants, an estimate of the vibrational frequencies of the transition state is required, which in turn requires some insight into the reaction mechanism. Since the threshold energy obtained with eq 1 can be considered as an upper limit to the true activation energy, one can rule out any contribution from reaction 1a to the immonium ion appearance curve, at least in the onset region. On the basis of this result, reaction 1b was taken as an initial guess of the actual reaction mechanism. The first step in reaction 1b involves intramolecular proton transfer between the amino nitrogen and the hydroxyl group, which probably proceeds via a five-membered proton-bridged ring intermediate. The energy barrier for this process is expected to correspond to the thermochemical barrier of 43 kcal/mol obtained by Bouchoux and Hoppilliard.^{17a} The next step involves the loss of H_2O from **Ic**. This process was modeled with low-level *ab initio* calculations (3-21G), see Figure 3. With **Ic** as the starting geometry, the C—OH₂ bond length was systematically increased while the remaining degrees of freedom were optimized. Lengthening the bond leads to a slight increase in energy (relative to **Ic**), reaching a maximum of 1.4 kcal/mol at 2.4 Å (see **Id**).¹⁸ Increasing the bond length to 2.5 Å (**Ie**) results in a large drop in energy, -14 kcal/mol relative to **Ic**.¹⁸ This drop in energy coincides with the C—C bond increasing from 1.52 to 2.64 Å, indicating that the acylium ion is no longer sufficiently stabilized by the water molecule and that the C—C bond dissociates such that **Ie** resembles a hydrated immonium ion, weakly associated with a CO molecule. Subsequent dissociation of **Ie** into the final products is exothermic, see Figure 3. By using the vibrational frequencies of **Id** (shown in Table 2) to represent those of the transition state, a threshold energy of 43.9 kcal/mol is obtained, see Table 1, which is in excellent agreement with the energy barrier predicted for the reaction proceeding via **Id**, based on Hoppilliard's value of 43 kcal/mol for the formation of **Ic** followed by a ~1 kcal/mol increase predicted by 3-21G for the formation of **Id**. The kinetic shift for this reaction is quite small, 0.5 kcal/mol, see Table 1.



The immonium and the immonium hydrate ions are seen to have similar threshold energies, Figure 2. Unfortunately, the intensity of the hydrate in the threshold region is too low to provide a reliable threshold fit (eq 1). The immonium hydrate is probably also produced by the transition state **Id**. The very rapid increase of the C—CO distance from **Id** to **Ie** while the OC—OH₂ distance remains almost the same indicates that most of the energy released when the reaction proceeds past the transition state involves relative motion of the CO group and is released as kinetic energy. Under these conditions, some H_2O molecules may be retained close to the immonium ion as ion-dipole type complexes. This would be particularly the case for precursor ions whose energy is equal to or only slightly above

(18) The HF energies (in atomic units) calculated with a 3-21G basis set are the following: $E(\text{Ic}) = -281.552329$, $E(\text{Id}) = -281.55077$, $E(\text{Ie}) = -281.574730$.

Table 2. Vibrational Frequencies (cm⁻¹) of Precursor Ions and Transition States (TS) Leading to a Given Fragment Ion

(Gly)H ⁺ ^a /TS ^d (H ₂ N=CH ₂ ⁺)	(GlyNH ₂)H ⁺ ^a /TS ^d (H ₂ N=CH ₂ ⁺)	(GlyNHMe)H ⁺ ^b / TS ^d (H ₂ N=CH ₂ ⁺)	TS/ y ₁ (⁺ H ₃ N-CH ₃)	(Gly)H ⁺ ^a /TS ^d (H ₂ N=CH ₂ ⁺)	(GlyNH ₂)H ⁺ ^a /TS ^d (H ₂ N=CH ₂ ⁺)	(GlyNHMe)H ⁺ ^b / TS ^d (H ₂ N=CH ₂ ⁺)	TS/ y ₁ (⁺ H ₃ N-CH ₃)						
100	-108	106	-135	60	-143	-516	1957	2470	1827	1869	1356	1330	1326
227	107	304	62	70	36	31	3277	3265	1852	1876	1359	1334	1337
320	121	358	86	79	77	54	3323	3327	1904	2440	1383	1342	1344
508	176	513	141	154	135	84	3346	3765	3119	3262	1412	1364	1368
561	206	523	234	237	152	128	3572	3829	3280	3358	1451	1379	1380
680	373	648	296	392	198	151	3621	3886	3347	3586	1625	1457	1436
698	388	703	341	432	228	257	3810	3942	3597	3704	1640	1522	1466
883	463	836	433	497	302	413			3651	3707	1651	1692	1666
994	468	838	509	585	318	432			3738	3777	1655	1712	1726
1011	496	1003	546	685	472	456			3854	3904	2002	2338	2352
1230	626	1014	583	927	500	679					2976	2921	2932
1235	753	1218	782	956	615	954					2998	2987	2973
1247	974	1229	961	1100	788	981					3005	2989	2990
1420	1198	1257	1195	1122	923	1016					3034	3011	3011
1473	1336	1435	1318	1152	1013	1025					3088	3094	3090
1560	1476	1463	1331	1200	1049	1039					3088	3396	3096
1609	1485	1532	1496	1239	1139	1099					3222	3455	3412
1709	1595	1618	1507	1273	1249	1234					3332	3482	3413
1825	1823	1668	1596	1319	1254	1237					3488	3512	3472
1850	1824	1816	1815	1350	1279	1270							

(Gly-Gly)H ⁺ ^b /TS ^d (H ₂ N=CH ₂ ⁺)	(Gly ₂ NH ₂)H ⁺ ^b / TSe (b ₂)	(Gly-Gly-Gly)H ⁺ ^c	(Gly-Gly)H ⁺ ^b /TS ^d (H ₂ N=CH ₂ ⁺)	(Gly ₂ NH ₂)H ⁺ ^b / TSe (b ₂)	(Gly-Gly-Gly)H ⁺ ^c					
25	-226	46	-17	24	1716	1336	1282	1267	1218	958
49	60	69	25	47	1727	1646	1298	1288	1267	980
73	93	84	97	59	2075	1372	1318	1331	1296	1014
95	96	129	115	63	2086	1399	1328	1361	1305	1063
149	123	226	125	79	2089	1421	1345	1382	1317	1096
238	154	258	179	82	3207	1435	1407	1412	1323	1128
282	207	305	220	92	3218	1568	1441	1422	1347	1160
349	262	356	225	183	3231	1623	1469	1581	1408	1193
412	298	434	266	214	3262	1628	1606	1586	1460	1229
508	326	457	369	260	3277	1644	1701	1630	1570	1262
521	417	493	372	285	3277	1648	1711	1636	1716	1286
538	489	564	407	310	3347	2002	2036	1657	1751	1305
582	516	569	508	327	3378	2072	2329	1702	1755	1318
587	534	600	519	350	3463	2956	2890	1953	1757	1386
652	538	623	577	385	3575	2966	2956	2025	2089	1397
687	622	698	650	417	3582	3026	2960	2968	2630	1412
935	634	764	55	441	3940	3028	3030	2984	2959	1419
946	656	918	711	500		3113	3345	3040	2969	1422
1031	930	952	801	513		3218	3399	3052	3035	1457
1059	953	969	941	593		3325	3452	3101	3406	1464
1122	958	1053	970	620		3397	3464	3198	3434	1480
1168	1010	1081	1002	630		3452	3499	3327	3437	1483
1203	1142	1174	1023	673				3452	3454	1603
1239	1146	1177	1079	681				3468	3478	1672
1275	1175	1207	1142	750						1703
1288	1275	1232	1155	948						

^a Vibrational frequencies were obtained from HF calculations with use of a 3-21G basis set. ^b Vibrational frequencies were obtained from semiempirical calculations (AM1). ^c The vibrational frequencies of (Gly-Gly-Gly)H⁺ were taken from a single local minimum obtained from semiempirical calculations (MNDO). ^d The vibrational frequencies of the transition state leading to the immonium ion were obtained from HF calculations (3-21G) for the precursor ions of GlyH⁺ and GlyNH₂H⁺ and from semiempirical calculations (AM1) for GlyNHCH₃H⁺ and (Gly-Gly)H⁺. Negative frequencies correspond to imaginary frequencies. ^e The vibrational frequencies of the transition state leading to the **b**₂ ion were obtained from semiempirical calculations (AM1). ^f The vibrational frequencies for the transition state (**VIc**) for the formation of the **y**₁ ion from GlyNHCH₃H⁺ were obtained from semiempirical calculations (AM1).

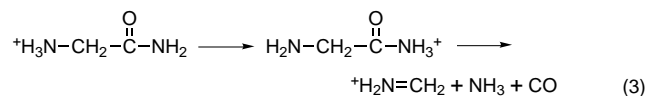
the energy of the transition state and is consistent with the observed absence of increase of the immonium hydrate intensity past the threshold region, see Figure 2. The bond distance changes from **Id** to **Ie** and the above interpretations are also consistent with the observed sizable kinetic energy releases, $T_{1/2} \sim 0.38$ eV (immonium)^{4a} and $T_{1/2} \sim 0.46$ eV (immonium hydrate),^{16b} when these ions are formed from the protonated amino acid.

Formation of the immonium ion is an example of a charge directed process, where the proton catalyzes bond dissociation. Charge remote fragmentation processes, in which simple homolytic bond cleavage occurs, require substantially higher internal energies. For example, C-C bond cleavage, which occurs in the formation of the ylide cation (⁺H₃N-CHO₂^{*}), is

expected to have a threshold energy of ~ 90 kcal/mol (based on the average C-C bond energy). The observed onset energy of the ylide ion in Figure 2 is above 6 eV (140 kcal/mol). This onset energy is likely artificially high due to a significant kinetic shift that can be attributed to lifetime effects, *i.e.* kinetic shift, combined with kinetic suppression of this pathway by the much faster competing reaction leading to the immonium ion.

The threshold curve obtained for the formation of the immonium ion from protonated glycine (**IIa**) is shown in Figure 4. The CID behavior of protonated glycine is similar to that observed for glycine. Low collision energies lead almost exclusively to the formation of the immonium ion, along with a small amount of the (⁺H₂N=CH₂)NH₃ complex. Formation of the immonium ion likely proceeds by the same

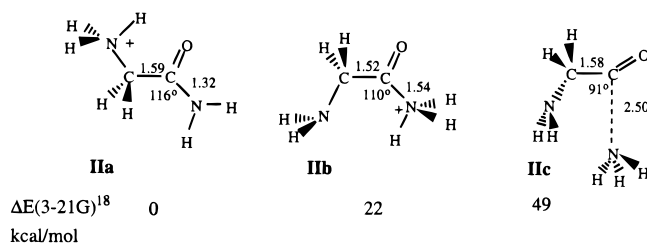
mechanism as proposed for glycine, namely proton transfer from the amino group to the amide nitrogen followed by the loss of NH_3 and CO (reaction 3).



As was the case for the amino acids, a large kinetic energy release, $T_{1/2} = 0.30\text{--}0.37$ eV, is associated with the immonium ions formed by the decomposition of protonated amino amides.^{4a}

On the basis of the relative energies of **IIa** and **IIb**, calculated at the 3-21G level in the present work, the energy increase for the proton transfer from the amino group to the amide nitrogen is ~ 22 kcal/mol,¹⁹ much smaller than the 43 kcal/mol for the corresponding proton transfer in glycine. A much smaller energy is expected for the amide because the transfer is to an amino group whose gas-phase basicity is expected to be much higher than that of the hydroxy group in glycine.

Protonation of the amide nitrogen results in lengthening of the C(O)–N bond, from 1.32 to 1.54 Å, indicating that the bond is weakened but much less so than the C(O)–O bond in glycine, which extended to ~ 2 Å on protonation of the hydroxy oxygen. In order to estimate the transition state structure, the loss of NH_3 from **IIb** was modeled, see Figure 5, using the same approach as described for glycine. The calculated energy (relative to **IIb**) is found to increase with increasing C– NH_3 bond length, reaching a maximum of 27 kcal/mol at a bond length of 2.5 Å (**IIc**).¹⁹ The energy at larger distances is found to decrease rapidly, coinciding with a rapid increase of the C–CO distance.



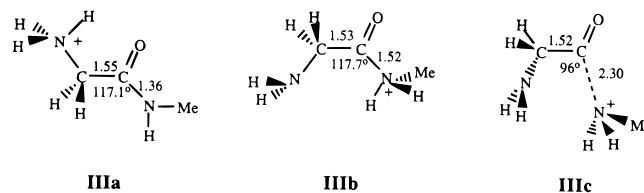
Using the vibrational frequencies of **IIa** and **IIc** (see Table 2) to represent the precursor ion and transition state, a threshold energy of 44.2 kcal/mol is obtained from the threshold curve, Figure 4, and fitting with eq 2. The kinetic shift for this reaction is 0.7 kcal/mol and thus very close to the 0.5 kcal/mol obtained for glycine, Table 1. The threshold value $E_0 = 44.2$ kcal/mol, which gives the energy change between **IIa** and the transition state **IIc**, should represent a more accurate value than the low-level theoretical result¹⁸ of 49 kcal/mol given above for **IIc**.

It is interesting that the transition state energies for the formation of the immonium ion from protonated glycine and glycylglycine are so similar, 43.9 and 44.2 kcal/mol, despite the large differences in the energies involved in the first step, *i.e.* the proton transfer reaction, which for glycine is more endothermic by some 21 kcal/mol owing to the lower basicity of the hydroxyl relative to the amino group. For the second step, which involves cleavage of the C–XH bond, the difference in endothermicity is exactly opposite. NH_3 is a better Lewis base and thus better able to bond to the acylium ion compared with H_2O , and therefore a larger energy is required to break the C– NH_3 bond. This compensation, leading to very similar total energies for the formation of the transition state, is due to an

(19) The HF energies (in atomic units) calculated with a 3-21G basis set are the following: $E(\text{IIa}) = -261.9110653$, $E(\text{IIb}) = -261.876203$, $E(\text{IIc}) = -261.8330618$.

expected positive correlation between the Brønsted and Lewis basicity of the leaving group. That an almost exact compensation results is somewhat surprising and must be a special case for the type of reaction that occurs.

The threshold curves obtained for the formation of the major fragment ions from protonated glycine methylamide (**IIIa**) are shown in Figure 6. CID of **IIIa** at low collision energies leads to the immonium ion as the major product and protonated methylamine, ${}^+\text{H}_3\text{NCH}_3$, as the minor product. The geometry and corresponding vibrational frequencies of **IIIa** were evaluated from semiempirical calculations (AM1). By using eq 1 to fit the appearance curves, the immonium ion and protonated methylamine are found to have similar threshold energies, 60.0 and 59.8 kcal/mol, respectively. The kinetic shifts associated with the production of these two ions are expected to be somewhat larger than those for glycine and glycylglycine due to the extra degrees of freedom introduced by the presence of the methyl group. We shall model the transition state and evaluate the kinetic shift for the immonium ion here. The ${}^+\text{H}_3\text{NCH}_3$ ion, which can be considered as a y type ion, will be examined in section c.



The transition state leading to the immonium is expected to be similar to that determined for glycylglycine. The geometry of the transition state (**IIIc**) was obtained from semiempirical calculations (AM1) used to model the loss of H_2NCH_3 from **IIIb**,²⁰ following the same procedure as for glycine and glycylglycine. By using the calculated frequencies of **IIIc**, a threshold energy of 49.9 kcal/mol is obtained with eq 2. This value is quite close to the threshold energy measured for glycylglycine, 44.2 kcal/mol, and is consistent with both reactions occurring via the same type of mechanism. The energy for the transition state **IIIc** relative to that of **IIIa**, evaluated with the AM1, was 34 kcal/mol. This is significantly lower than the threshold energy of 49.9 kcal/mol. The AM1 approach energy is probably in error. This is also indicated by the AM1 predicted energy for the transition state for protonated glycylglycine **IIc** relative to **IIa** which was 34 kcal/mol, while 3-21G had predicted 49 kcal/mol, in closer agreement with the threshold value of 44.2 kcal/mol.

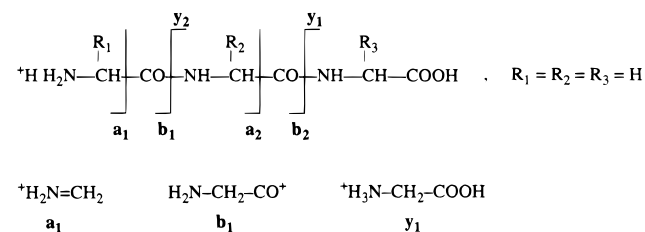
The degree to which the kinetic shift is sensitive to the number of degrees of freedom can be seen by comparing the results obtained for glycylglycine and glycylglycine methylamide. Replacing a hydrogen with a methyl group causes the kinetic shift to increase from 0.7 kcal/mol for glycylglycine to 10.1 kcal/mol for glycylglycine methylamide, Table 1.

b. CID of Protonated Glycylglycine and Glycylglycylglycine. Mechanism and Transition State Energies for Formation of \mathbf{a}_1 , \mathbf{a}_2 , and \mathbf{b}_2 Ions. The peptide sequencing notation,⁴ Scheme 2, for fragment ions will be used in the subsequent discussion.

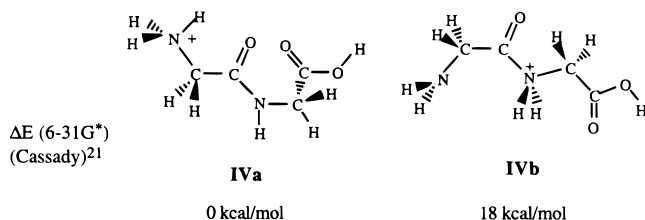
CID of the protonated dipeptide, glycylglycine (Gly-Gly), results exclusively in the formation of the \mathbf{y}_1 (protonated glycine) and \mathbf{a}_1 (immonium ion) fragment ions at energies less than 50 eV (lab). From the appearance curves, shown in Figure 7, it can be seen that the \mathbf{y}_1 ion has the lower onset energy, but that at higher energies the \mathbf{a}_1 ion becomes the dominant fragment

(20) The calculated AM1 energies (in atomic units) are the following: $E(\text{IIIa}) = -45.423633$, $E(\text{IIIb}) = -45.410295$, $E(\text{IIIc}) = -45.37007$.

Scheme 2



ion. HF calculations (6-31G*) carried out by Cassady *et al.*²¹ predict that the protonated amide nitrogen species (**IVb**) is 18 kcal/mol less stable than the terminal amino protonated structure (**IVa**).

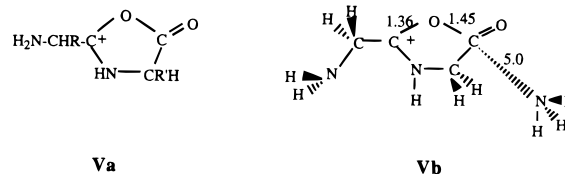


AM1 calculations were used to locate the transition state for the formation of the unstable acylium **b**₁ ion whose spontaneous decomposition, see preceding section, leads to the immonium ion **a**₁. The transition state for the unstable **b**₁ ion was similar to structures **IIc** or **IIIc**, but with glycine as the leaving neutral group. At the AM1 level of calculation, the transition state was predicted to lie 17 kcal/mol higher in energy than the amide protonated form **IVb**. The vibrational frequencies obtained for the subsequent transition state are given in Table 2. From the appearance curve and the evaluated frequencies, a threshold energy of 43.7 kcal/mol (eq 2) is obtained for the formation of the **a**₁ ($H_2N=CH_2^+$) ion. This value can be compared with the very approximate theoretical estimate of ~35 kcal/mol based on the energy changes for the proton transfer (6-31G*) of 18 kcal/mol and the AM1 value for the transition state formation of 17 kcal/mol. The $E_0 = 43.7$ kcal/mol value from the threshold measurement is quite close to the energies obtained for the related decompositions where glycylglycine and *N*-methylglycylglycine produce the $H_2N=CH_2^+$ ion: $E_0 = 44.2$ kcal/mol and $E_0 = 49.9$ kcal/mol, Table 1. Since these reactions are similar, close lying E_0 values are expected. The kinetic shift for the present reaction is large, 20 kcal/mol, and represents close to one third of the threshold energy evaluated without correction for the kinetic shift, $E_0 = 60$ kcal/mol, eq 1. Obviously, the major source of uncertainty in the threshold energies even for these small biomolecules lies in the modeling of the transition state and the evaluation of the kinetic shift.

The appearance curves of the dominant CID fragment ions generated from protonated glycyglycylglycine (Gly-Gly-NH₂) are shown in Figure 8. The most striking feature of the breakdown graph is the very low onset energy for the ion produced by the loss of NH₃ (m/z 115). By using eq 1 to fit the data, a threshold energy of 21.4 kcal/mol is obtained. The ion (m/z 115) should be the **b**₂ ion ($H_2NCH_2CONHCH_2CO^+$), yet the threshold energy is much lower than the threshold energies of 45–50 kcal/mol, Table 1, for the formation of the unstable acylium **b**₁ ions which led to the **a**₁ ions from protonated glycylglycine, methylglycylglycine, and glycyglycine. The very low energy for the **b**₂ ion suggests that this ion does not have the acylium structure but a structure that is stable and

of lower energy. This observation is fully substantiated by the recent proposal of Harrison and co-workers,^{4a} who found that the loss of HX was the dominant dissociation process in the metastable spectra of FAB-generated peptides with the general structure ${}^+H(H_2NCHRCONHCHR'CO-X)$, where X = OH, NH₂, Gly, and Ala and the side groups (R) were the hydrogen atom or alkyl groups. More importantly, the loss of XH was not accompanied by the loss of CO as observed in the analogous reactions involving protonated glycine or glycylglycine, *i.e.* for these species, the **b**_{*n*} type ions were relatively stable and did not decompose completely to an **a**_{*n*} ion and CO. Harrison^{4a} proposed that the **b**₂ ion is not acyclic as is the case for the **b**₁ ion obtained from glycine and glycylglycine, but is stabilized due to a cyclization leading to protonated oxalzone, see structure **Va** below. Theoretical calculations which showed that the cyclic structure **Va** is more stable by ~34 kcal/mol than the acyclic acylium ion structure provided additional support for this proposal.^{4a}

In order to determine the kinetic shift-corrected threshold energy for the **b**₂ ion, the vibrational frequencies of the transition state **Vb** were evaluated semiempirically,²² Table 2. By using these frequencies and the threshold curve, Figure 8, a threshold energy of 20.4 kcal/mol, Table 1, is obtained.



The energy difference between the transition state **Vb** and the terminal amino group protonated Gly-Gly-NH₂, evaluated with the semiempirical AM1 method, is ~27 kcal/mol. This value is not too far from the activation energy $E_0 = 20.4$ kcal/mol obtained from the threshold (eq 2) determination and is in support of the oxalzone mechanism. It is very desirable to evaluate the activation energy with high-quality *ab initio* calculations and compare it with the experimental $E_0 = 20.4$ kcal/mol result. An agreement between the two results will constitute a strong support for the oxalzone mechanism.^{4a}

Harrison *et al.*^{4a} also found that dissociation of energized cyclic **b**₂ ions occurs by loss of CO to give the corresponding **a**₂ ion. The kinetic energy release determined^{4a} for this reaction was quite large, $T_{1/2} \approx 0.5$ eV. On the basis of calculations, the authors predicted that the loss of CO from the oxalzones proceeds via ring opening to give the acyclic acylium ion, from which loss of CO is exothermic. For the **b**₂ ion, $HCONHCH_2CO^+$, the energy barrier associated with ring opening and loss of CO was calculated to be 1.49 eV, or 34 kcal/mol.^{4a}

CID of protonated Gly-Gly-NH₂ leads also to formation of an **a**₂ ion, $H_2NCH_2CONHCH_2^+$, with a threshold energy of $E_0 = 69$ kcal/mol (eq 1, Table 1, Figure 8). The transition state was not modeled, and we are not able to say whether the threshold energy is consistent with a direct dissociation mechanism via the acylium ions analogous to the mechanism for the formation of the **a**₁ ions from the glycylglycines, or a mechanism which involves formation of an excited oxalzone followed by oxalzone ring opening and loss of CO.

The formation of a stable **b**₂ ion was not observed for protonated Gly-Gly, Figure 7. The proton transfer from the terminal NH₂ to the OH group requires a very much higher

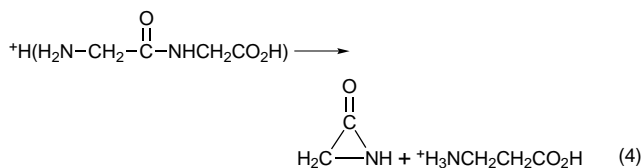
(21) Zhang, K.; Zimmerman, D. M.; Chung-Phillips, A.; Cassady, C. J. *J. Am. Chem. Soc.* **1993**, *115*, 10812.

(22) The geometry of the **Vb** was obtained, using semiempirical calculations (AM1), by varying the C–NH₃ bond length and optimizing the remaining degrees of freedom. The energy maximum ($E = -69.993005$ au) was located at a bond length of 5.0 Å.

energy than is the case for Gly-Gly-NH₂; see the analogous case for glycines: structures **Ia**, **Ic** and **IIa**, **IIb**. On this basis, the formation of the **b**₂ ion from Gly-Gly-OH would require a much higher threshold energy E_0 . One might consider that this higher energy might be inducing the complete decomposition of the **b**₂ ion to the **a**₂ ion, but the formation of an **a**₂ ion is not observed for Gly-Gly, Figure 7. Notably, formation of **a**₂ is observed for Gly-Gly-NH₂ at the expected higher energy, Figure 8. The question why an **a**₁ ion is observed but an **a**₂ ion is not observed from Gly-Gly, even though the two dissociations might require very similar activation energies, can be answered by the following proposed explanation. The formation of the **a**₁ ion requires the initial protonation of the amide nitrogen which is of much lower energy than the protonation of the OH group required for the **a**₂ ion formation. Endothermic proton transfer by proton bridged cyclic intermediates to basic sites such as amide nitrogens may be expected to be very much faster than the subsequent transition state formation. So much so that a quasiequilibrium of protonated sites with different basicities may be expected. Under such a condition a very much faster decomposition may be expected from the site with the higher basicity (*i.e.* amide nitrogens) than the site at low basicity (*i.e.* OH), even when the activation energies for the two decompositions are the same. Therefore, for Gly-Gly, the decomposition from the protonated amide group will be much faster than the decomposition from the OH protonated group and the formation of the **a**₂ ion will be suppressed.

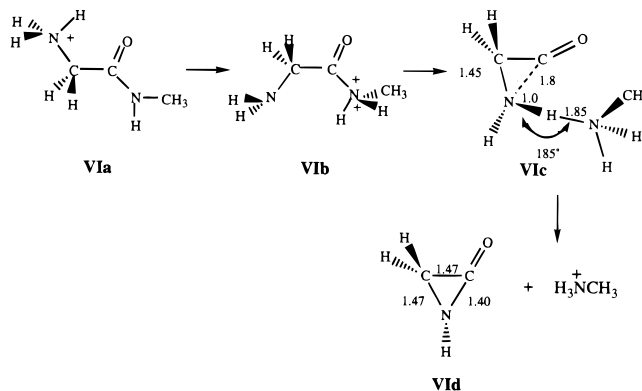
c. Mechanism and Transition States for the Formation of **y₁ Ions from Protonated Glycine Methylamide, Glycylglycine, and Glycylglycinamide.** A **y**₁ type ion (protonated glycine), see Scheme 2, is obtained from CID of protonated Gly-Gly-OH, Figure 7, and Gly-Gly-NH₂, Figure 8. Formation of a **y** type ion involves the transfer of a proton and a hydrogen atom to the amide nitrogen. The protonated methylamine product ion observed from CID of protonated glycine methylamide, see Figure 6, can also be considered as an **y**₁ ion.

Based on CID experiments carried out on (Phe-Phe-Phe-(d₅)+D)⁺, Mueller *et al.*²³ concluded that the transferred hydrogen associated with the formation of the **y** ions from the CID of protonated peptides originates from the nitrogen on the N-terminal side of the cleavage site. Additional insight into this reaction has been obtained from neutralization-reionization mass spectrometry experiments, carried out by Cordero and co-workers,¹⁶ which identified the neutral that is lost in the formation of the **y**₁ ion from (Ala-Ala)H⁺ as a cyclic aziridinone molecule. The aziridinone neutral expected in the formation of the **y** ion, ⁺H₃N-CH₂CO₂H, from CID of protonated glycylglycine is shown below:



To our knowledge, no detailed evaluation of the mechanism and transition state leading to the **y**₁ ion has been reported. In the absence of a more detailed analysis, we propose the mechanism shown in Scheme 3, which is written for glycyl methylamide. Replacing the CH₃ with CH₂CO₂H or CH₂-CONH₂ would lead to the proposed scheme for glycylglycine or glycylglycinamide. Semiempirical calculations with AM1 were used to locate the transition state **VIc**. Intermediate

Scheme 3



structures between the amide protonated structure **VIb** and the transition state **VIc** were evaluated, which represented the gradual cyclization and the simultaneous cleavage of the carbonyl carbon to the amide nitrogen bond. These structures showed that the transition is assisted by the hydrogen bond seen in the transition state and this hydrogen bond also leads to the second hydrogen transfer required for the formation of the final products. The energy of the transition state **VIc** relative to **VIa** was predicted as 49 kcal/mol while the overall reaction endothermicity was 51 kcal/mol. The transition state was selected at **VIc** because this state is more entropically constrained than the slightly more endothermic transition to the products **VIa**. The vibrational frequencies of the transition state **VIc**, see Table 2, were used to fit the **y**₁ ion threshold curve, see Figure 6, and a threshold energy of $E_0 = 48.5$ kcal/mol ($n = 1.08$) was obtained. This threshold value together with ΔS^\ddagger are given in Table 1. The threshold energy happens to agree very closely with the AM1 evaluated energy of the transition state of 49 kcal/mol; however, this close agreement is not very significant since the energy predictions of the AM1 method are not reliable to within several kcal/mol—see previous results for the immonium ion.

A threshold energy of 49.9 kcal/mol for the **y**₁ ion is also shown in Table 1. This value was obtained by fitting the **y**₁ ion threshold curve, Figure 6, with eq 2 and the frequencies for the transition state for the formation of the **a**₁ ion (Table 2). This result illustrates that the threshold energy is not very sensitive to the exact values of the frequencies used when the entropies of the transition states are fairly similar, as is the case here ($\Delta S^\ddagger = 4.6$ cal/(deg mol) for **y**₁ and 5.8 cal/(deg mol) for **a**₁), see Table 1.

The thresholds for the **y**₁ ion formation from protonated Gly-Gly could not be fitted with eq 2 because no calculations for the transition state frequencies were performed. The threshold for the **y**₁ ion from Gly-Gly, $E_0 = 54.1$ kcal/mol (eq 1), is lower than that for Gly-NHCH₃, $E_0 = 59.8$ kcal/mol (eq 1), and since the kinetic shift for Gly-Gly is expected to be larger, the kinetic shift corrected E_0 for **y**₁ ion formation from Gly-Gly is expected to be close to 10 kcal/mol lower than the $E_0 = 48.5$ kcal/mol, eq 2, value for Gly-NHCH₃. Assuming that Gly-Gly decomposes by a transition state similar to that for **VIc**, the question arises, why are the energies so different? It is possible that for Gly-Gly, the carbonyl group of the C terminus provides some stabilization by H bonding to the bridging proton in the **VIc** analogous structure and in the formation of the protonated product **y**₁ ion. Such an assistance could lower the transition state energy by several kcal/mol, although an adverse entropic change will reduce somewhat the overall effect.

The thresholds (eq 1) for **y**₁ and **a**₁ from Gly-GlyNH₂, $E_0(\mathbf{y}_1) = 69$ kcal/mol and $E_0(\mathbf{a}_1) = 82$ kcal/mol, are much higher

(23) Mueller, D. R.; Eckersley, M.; Richter, W. J. *Org. Mass Spectrom.* **1988**, *23*, 217.

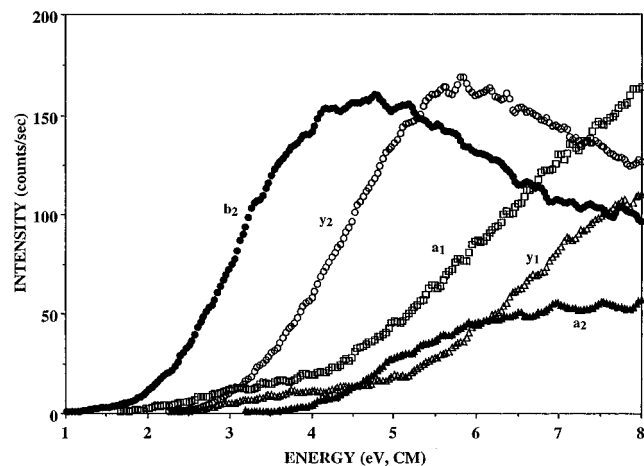


Figure 9. Appearance curves of the \mathbf{b}_2 (●), \mathbf{y}_2 (○), \mathbf{a}_2 (▲), \mathbf{a}_1 (□), and \mathbf{y}_1 (△) fragment ions from CID of (Gly-Gly-Gly) H^+ .

than the corresponding thresholds for Gly-Gly, $E_0(\mathbf{y}_1) = 54.1$ kcal/mol and $E_0(\mathbf{a}_1) = 64.9$ kcal/mol, Table 1. This large difference is probably due to a competitive kinetic shift, *i.e.* the effect of the much faster low threshold reaction leading to \mathbf{b}_2 ions for Gly-GlyNH₂, which kinetically suppresses the other dissociation reactions.

d. Threshold Curves for Protonated Gly-Gly-Gly and Gly-Gly-Gly-Gly. The CID threshold graph of protonated Gly-Gly-Gly is shown in Figure 9. The \mathbf{b}_2 ion is again found to be formed in the lowest energy process. However, the onset energy, 54.5 kcal/mol (eq 1),²⁴ is considerably higher than that measured for glycylglycinamide (21.4 kcal/mol). Although we have not attempted to model the kinetic shift for this reaction, this increase of some 33 kcal/mol in the observed threshold energy is believed to reflect not a change in activation energy but an increase in the kinetic shift due to the addition of the extra glycine residue.

The \mathbf{a}_1 ion, which has the second lowest onset energy, exhibits a relatively small cross section up to ~ 4.5 eV. Above this energy the cross section increases much more rapidly with collision energy, indicating that additional reaction pathways are contributing to the ion intensity. This is expected since the immonium ion (\mathbf{a}_1) is a major decomposition product of all of the larger fragment ions.

At a collision energy of approximately 2.5 eV, the onset of the \mathbf{y}_1 and \mathbf{y}_2 ions is observed. Initially, the \mathbf{y}_2 ion cross section increases much faster with collision energy compared to the \mathbf{y}_1 ion. The neutral lost in the formation of the \mathbf{y}_2 will be the aziridinone as previously discussed. In the case of the \mathbf{y}_1 ion, the hydrogen atom that is transferred can originate either from the terminal nitrogen or from the adjacent amide nitrogen. The neutral that is formed will then correspond to either a diketopiperazine or a substituted aziridinone molecule. There is experimental evidence that the diketopiperazine, which is expected to be thermodynamically more stable than the tight three-membered cyclic aziridinone, is in fact the neutral that is lost in the formation of the \mathbf{y}_1 ion from tripeptides.¹⁶ The small initial cross section observed for the \mathbf{y}_1 ion is likely due to the much faster reaction occurring at that same amide bond leading to the \mathbf{b}_2 ion. At ~ 5 eV one observes a sharp increase in the

(24) No detailed search for the lowest energy geometry of protonated Gly-Gly-Gly was performed; the internal energy distribution of the precursor ion was evaluated by using the vibrational frequencies of a single local minimum obtained from semiempirical calculations. The average internal energy obtained with these frequencies is 7.2 kcal/mol. This is close to what one would have estimated based on the average internal energies obtained for protonated glycine, 1.7 kcal/mol, and glycylglycine, 4.4 kcal/mol.

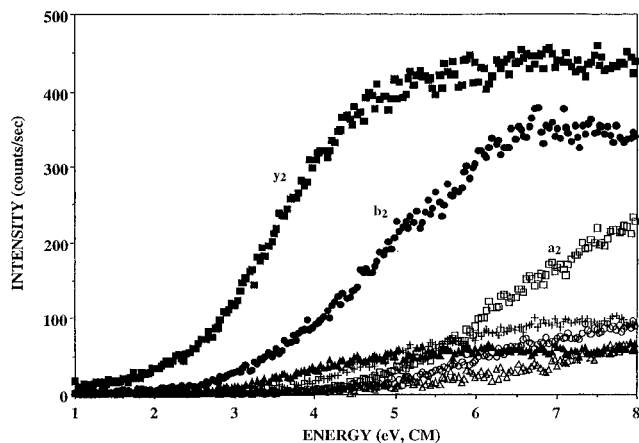


Figure 10. Appearance curves of the \mathbf{b}_2 (●), \mathbf{y}_2 (■), \mathbf{a}_2 (□), \mathbf{b}_3 (▲), \mathbf{y}_3 (+), \mathbf{a}_1 (△), and \mathbf{y}_1 (○) fragment ions from CID of (Gly-Gly-Gly-Gly) H^+ .

\mathbf{y}_1 appearance curve; this is due to the decomposition of \mathbf{y}_2 into \mathbf{y}_1 and \mathbf{a}_1 ions. By using eq 1 to fit the data, the \mathbf{y}_2 threshold energy is found to be 73.1 kcal/mol. Due to the kinetic shift and kinetic suppression of this pathway by the \mathbf{b}_2 reaction, this threshold energy substantially overestimates the true activation energy, which is expected to be < 38 kcal/mol, based on the glycylglycine results.

It is interesting to compare the relative ion abundances obtained from our low-energy experiments with those obtained from high-energy CID.²⁵ Under high-energy conditions, the \mathbf{b}_2 ion is found to be the dominant ion produced, with the only other significant fragment being the \mathbf{y}_2 ion. The relative ion abundances at high energy therefore correspond to what we observe at very low collision energies (see Figure 9). A survey of the high-energy CID spectrum of other protonated tripeptides reveals that the \mathbf{b}_2 and \mathbf{y}_2 ions are always observed as major fragment ions.

The largest system examined in the present work is protonated Gly-Gly-Gly-Gly, which contains three amide bonds at which cleavage can occur. The breakdown graph for this ion is shown in Figure 10. The two dominant low-energy fragment ions are the \mathbf{y}_2 and \mathbf{b}_2 ions which originate from cleavage of the middle amide bond. Somewhat surprisingly, it is the \mathbf{y}_2 ion that has the lowest observed onset energy, in contrast to what was observed with Gly-Gly-Gly. It is not clear whether this lower observed onset energy for the \mathbf{y}_2 ion is the result of a lower activation energy or whether this reflects faster dissociation kinetics (*i.e.* a smaller kinetic shift). The threshold energies of the \mathbf{y}_2 and \mathbf{b}_2 ions, determined by using eq 1, are 63 and 79 kcal/mol respectively.^{26,27} Also observed in the breakdown graph are the \mathbf{y}_1 , \mathbf{y}_3 , \mathbf{a}_1 , and \mathbf{b}_3 ions with similar onset energies. The reaction cross sections for these fragment ions are much lower than those observed for the \mathbf{b}_2 and \mathbf{y}_2 ions, suggesting much slower dissociation kinetics for cleavage of the amide

(25) Kulik, R. W.; Heerma, W. *Biomed. Environ. Mass Spectrom.* **1989**, *18*, 910.

(26) Since the vibrational frequencies for the precursor ion were not calculated, the E_0 values given in Table 1 were obtained by fitting the threshold curves in Figure 10 by eq 0, $\sigma = \sigma_0(E - E_0)^n/E$, for origin of equation see Armentrout.⁷ The threshold E_0 obtained with eq 0 was increased by the average internal energy of the precursor ion at 300 K, which was estimated to be 10 kcal/mol. This estimate was based on the thermal energies quoted above.²⁴ It has been our experience that when the vibrational frequencies were available and threshold values E_0 were obtained with eq 1, these values were well approximated by the threshold obtained with eq 0 augmented by the average internal energy. However, this does not seem to be the case always. For a contrasting example, see Schultz *et al.*²⁷

(27) Schultz, R. H.; Crellin, K. C.; Armentrout, P. B. *J. Am. Chem. Soc.* **1991**, *113*, 8590.

bonds at either end of the peptide compared with the middle bond. It is not clear why CID leads preferential cleavage at the middle amide bond, and this question deserves further investigation.

The relative ion abundances in Figure 10 differ substantially from those observed in the metastable^{4a} and CID²⁸ spectrum of the FAB-generated peptide. In both cases, the **y**₂ ion is observed as the major fragment ion; similar to our results, however, the **b**₄ and to a lesser extent the **b**₃ ions are also observed in large abundance. The **b**₄ ion, which is formed by the loss of H₂O, is especially interesting since we observe it only as a very minor fragment ion. Loss of H₂O is in fact a common process in the decomposition of FAB-generated polyglycines and alanines.^{4a,28} In our measurements also the **b**₃ ion was essentially absent in the Gly-Gly-Gly spectrum and the **b**₂ from the Gly-Gly spectrum. On the other hand, the **b**₂ ion was the major product from Gly-GlyNH₂, see Figures 7–9. The observation of a **b**₂ ion from the amide but not from the acid was attributed to the much lower endothermicity of the amide NH₂ relative to the OH protonation, see section b of the Discussion. The high abundance of **b**_{*n*} ions from the (Gly)_{*n*} acids observed with FAB ionization indicates that for some reason the FAB process produces a higher abundance of OH-protonated precursor ions.

IV. Conclusions

The present work details the first attempt to quantify the dissociation energetics of small protonated peptides with energy-resolved CID. At low collision energies (<10 eV, CM), ions with the general structure ⁺H(H₂N-CH₂-CO-X) are found to dissociate primarily at the C–X bond. For X = OH, NH₂, NCH₃, and NHCH₂COOH, the immonium ion (or **a**₁ ion) was observed as a major fragment ion. The energetics for this reaction were found to be relatively insensitive to the nature of X, with threshold energies lying between 44 and 50 kcal/mol. The threshold energies were found to be close to the theoretically evaluated activation energies for transition states which conform to a mechanism proposed by Harrison and co-workers.^{15b}

When X was NHCH₃ or NHCH₂COOH a second dissociation pathway is found to operate leading to XH₂⁺ (**y**₁) as the fragment ion. The threshold energies for that process were somewhat lower than the quoted energies for the **a**₁ ion. The transition

state for the **y**₁ formation from X = NHCH₃ was modeled on the basis of the aziridinone structure for the neutral product proposed by Wesdemiotis and co-workers¹⁶ and found in agreement with the threshold energy.

The lowest energy CID fragment ion observed for ions with the general structure Gly-Gly-NH₂ and Gly-Gly-Gly is found to be the **b**₂ ion, corresponding to the loss of neutral HX. In the case of glycyglycinamide, the threshold energy for this reaction was measured to be 20.4 kcal/mol. This very low threshold energy is consistent with the **b**₂ ions undergoing cyclization, leading to a protonated oxalzone structure, as proposed by Harrison and co-workers.^{4a}

While the agreement observed between the threshold energies and the theoretically evaluated activation energies for the above three reaction types is encouraging, theoretical evaluations at a much higher level are required for a convincing confirmation.

The observed onset energies for the fragment ions of precursors larger than glycineamide are found to be significantly affected by kinetic shifts. For example, the kinetic shift observed for the **a**₁ ion produced from glycine is 0.5 kcal/mol, while for glycyglycine it increases to 21 kcal/mol. An additional source of large kinetic shifts stems from the competitive nature of the dissociation processes that occur. Fast processes, with large relative rate constants, tend to kinetically suppress other pathways which may be energetically accessible but proceed at a slower rate. As a result of these two factors and the increasing difficulty to model the transition states involved, the uncertainty associated with CID threshold energies increases as the size of the ion and number of fragment ions increases.

Even though there appears to be a limitation to the size of peptide (up to and including tripeptide) that can lead to useful threshold determinations, much interesting work within this limitation remains to be done. This would involve residues other than glycine and particularly residues with basic groups which are known to affect strongly the fragmentation pathways.

Acknowledgment. The present work was supported by grants from the Canadian National Sciences and Engineering Research Council NSERC. The authors are indebted to Professor P. Armentrout for making the CRUNCH program available to them.

(28) Yeh, R. W.; Grimley, J. M.; Bursley, M. M. *Biol. Mass Spectrom.* **1991**, *20*, 443.